Transactions, SMiRT-22
San Francisco, California, USA - August 18-23, 2013
Division VI

DETAILED STUDY OF THE STEEL LINER NEAR THE EQUIPMENT HATCH OF A PRESTRESSED CONCRETE CONTAINMENT

Patrick Anderson[a], Oscar Elison[a] and Ola Jovall[a]

[a] Scanscot Technology AB, Sweden

ABSTRACT

It has been shown in containment pressure tests that the global displacement measured at liner failure does not correspond to the critical strain level for the liner. A general conclusion from these tests is that significant strain concentration has to take place to get this "early" liner failure. In this paper the detailed liner behavior in the region of the equipment hatch of a ¼ scale containment model (Sandia ¼) is studied by non-linear finite element models. An analysis approach with three levels of model discretization is used, where *level 1* regards the global concrete containment behavior, *level 2* regards the local liner-concrete interaction and *level 3* regards the detailed strain level in vicinity of a discontinuity. The results from this study show two typical regions with elevated liner strain; (1) in the vertical folds between the equipment hatch embossments and the general curved wall and (2) in sections where the wall hoop reinforcement is decreased. The elevated strain along the vertical fold arises due to the flexural behavior when the liner is straightened out at high internal pressure. The elevated strain in regions with decreased reinforcement arises due to decreased axial wall stiffness in these regions. In the Sandia ¼ pressure test, liner failures were detected in regions which agrees with elevated strain found in this paper.

INTRODUCTION

A substantial part of the concrete reactor containments in US and Europe are constructed with an inner steel liner which constitutes the ultimate leak-tightness barrier. The liner is not regarded as part of the load-bearing system of the containment, the liner acts mainly as a leak-tightness membrane. The liner is attached to the inner surface of the concrete containment by discrete anchors made up of studs or by continues structural shapes (e.g. L or T sections). In performed pressurization tests on scaled containment models, see e.g. Horschel D.S. et al. (1989) and Hessheimer M.F. et al. (2003) it have clearly been shown that the containment global deformation measured at liner failure do not correspond to the critical strains given for the liner material. To reach critical strain values in the liner substantial strain concentrations are a prerequisite.

The work presented in this paper is a part of Scanscot Technology´s contribution to the SPE round-robin project[1,2]. In this part of the SPE project the participants were asked to study the detailed behavior in the region of the equipment hatch (E/H) for a ¼ scale containment model tested by pressurization (Sandia ¼), see Hessheimer M.F. et al. (2003). In the Sandia ¼ test it was concluded that the first leakage was caused by liner tears found near the E/H embossment (see Figure 1).

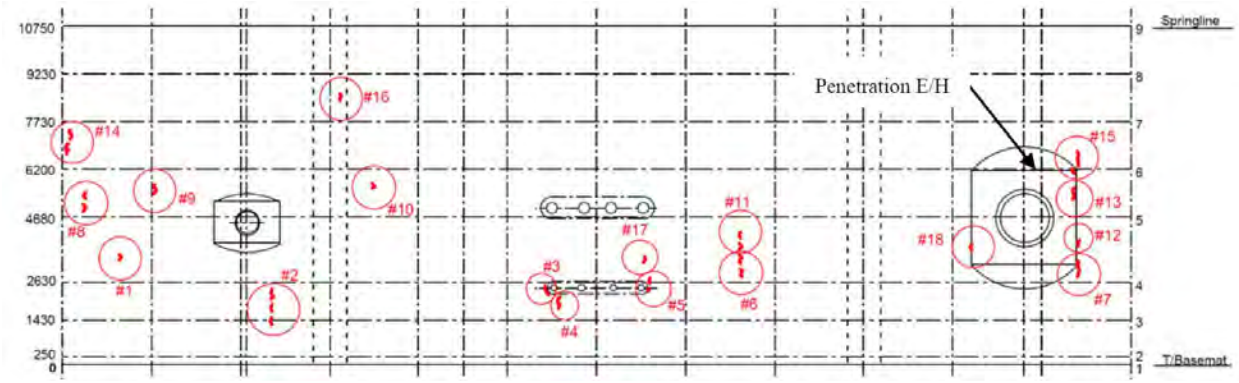

Figure 1. Stretched-out sketch, detected tears in the liner (Hessheimer M.F., 2003).

The detailed liner behavior in the region of the equipment hatch (E/H) is studied by finite element (FE) models describing the liner and the interaction with the concrete containment structure. An analysis approach with three levels of model discretization is used in this study (see Figure 2), where *level 1* regards the global concrete containment behavior, *level 2* regards the local liner - concrete interaction and *level 3* regards the detailed strain level in vicinity of a discontinuity.

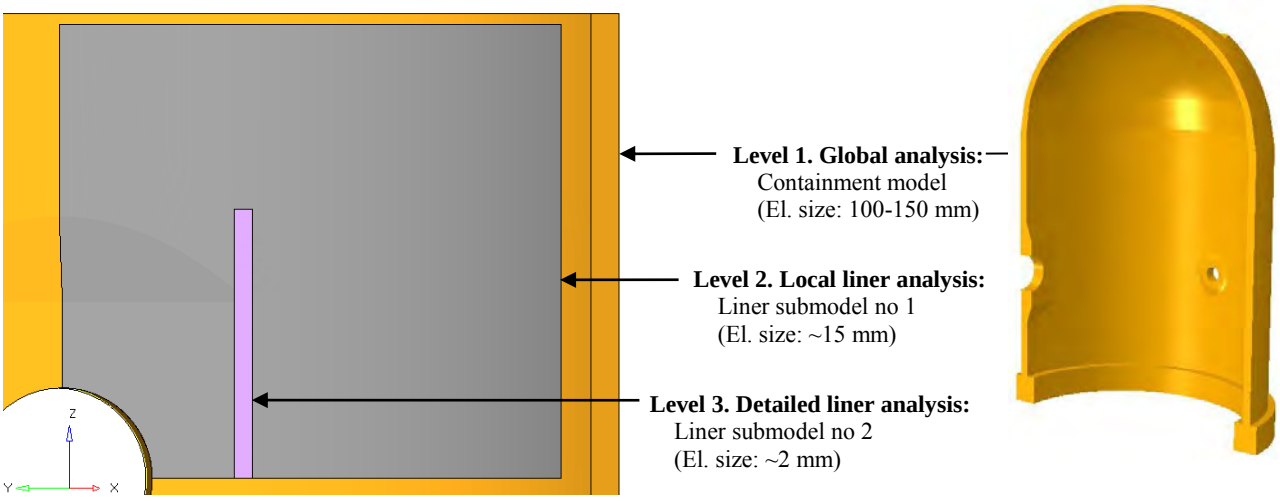

Figure 2. FE-modeling levels

[1] SPE, Standard Problem Exercise on the performance of containment vessels under severe accident conditions.
[2] Scanscot Technology´s participation in the SPE project was sponsored by Swedish/Finnish nuclear power industry and the Swedish Radiation Safety Authority (SSM).

The containment structural behavior is simulated up to failure and the FE-analyses[1] are therefore carried out using non-linear material models. To be able to simulate the interaction between concrete and steel components non-linear contact definitions are utilized. So called sub-modeling technique is utilized where a specified interface on the global model is defined and used as a displacement load for the liner sub-model. This technique is suitable for liner studies, as the liner can be seen as displacement controlled.

The global behavior of the Sandia ¼ containment structures where studied in the ISP48 project[2]. The basis of the modeling technique used by Scanscot Technology in ISP48[3] is adopted for the global model used in the study presented in this study. In Anderson (2008a) a study regarding the liner-concrete interaction in the E/H penetration region (Sandia ¼) is presented and a similar modeling approach is introduced in this study. The analysis of the liner is in this study improved by introducing sub-modeling technique, where the detailed deformation of the inner concrete containment surface is obtained from the global model. Also, a third discretization level is introduced capturing the local liner strain near discontinuities.

LINER FE-MODELS

The local liner model (level 2) is modeled with 4-node shell elements with reduced integration and the position is shown in Figure 3. The model describes ¼ of the liner in the region close to the E/H. The element size is around 15 mm.

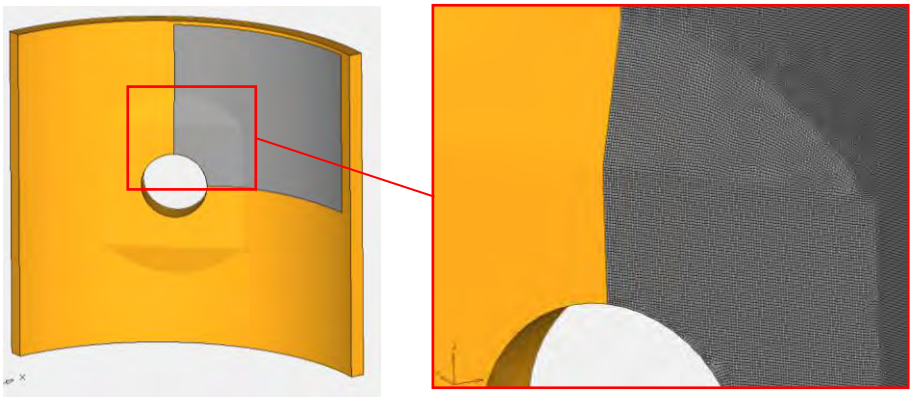

Figure 3. Position of local liner model (level 2).

[1] The analyses are carried out by the finite element program Abaqus/Explicit and Abaqus/Standard.
[2] International Standard Problem 48, Containment Capacity.
[3] See ISP48 (2005), appendice L.

The liner is anchored to the concrete via vertical T-anchors which are grouted into the concrete. The T-anchors are modeled with 2-node connector elements. The T-anchors have an in-plane shear stiffness in the circumferential direction, which is defined in the SPE project. The T-anchors are considered as rigidly connected to the concrete in the radial and vertical direction. Horizontal stiffeners are welded to the liner and also grouted into the concrete. The connection to the concrete is modeled with 2-node connector elements with an in-plane shear stiffness in the vertical direction, which is defined in the SPE project. The horizontal stiffeners are also modeled with shell elements (only connected to the liner elements) to include the added stiffness to the liner. Figure 4 shows the local liner model (level 2) with horizontal stiffeners and with the connector elements highlighted in yellow.

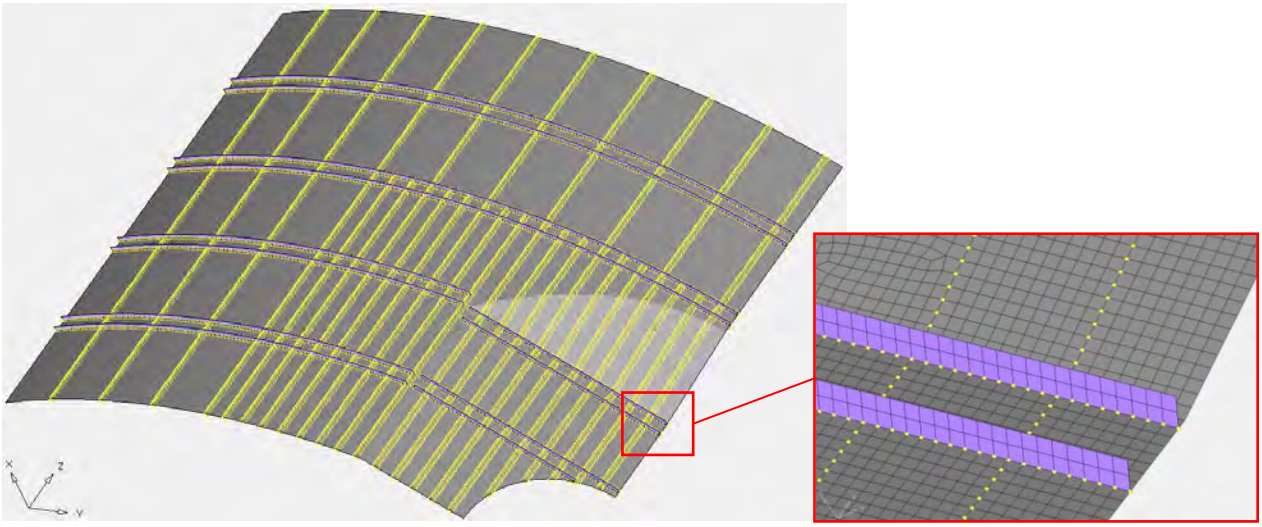

Figure 4. Liner FE-model with connectors highlighted in yellow and horizontal stiffeners modeled with shell elements.

The concrete inner surface in the local liner model is described by shell elements, where the displacements, given from the global FE-model, govern all nodes in the concrete shell. The liner shell is connected to the concrete shell via the connector elements, as described above. The surface interaction between the liner and concrete shell is described with an element based contact surface. The friction coefficient is assumed to be zero and the contact formulation allows for arbitrary separation, sliding, and rotation of the surfaces.

In the analysis it is shown that the narrow liner field along the vertical bend line, outlined in Figure 5, will straighten out between the vertical T-anchors when the containment wall expands due to the applied inner pressure. Consequently, high concentrations of stress and strain will develop in this region. Thus, a second sub-model (level 3) is generated modeling the liner field along the vertical bend line

which is confined between the vertical T-anchors, see Figure 5. This second sub-model has an increased element density and the general element size is 2 mm. The first sub-model (level 2) governs the boundary displacements of the second sub-model (level 3).

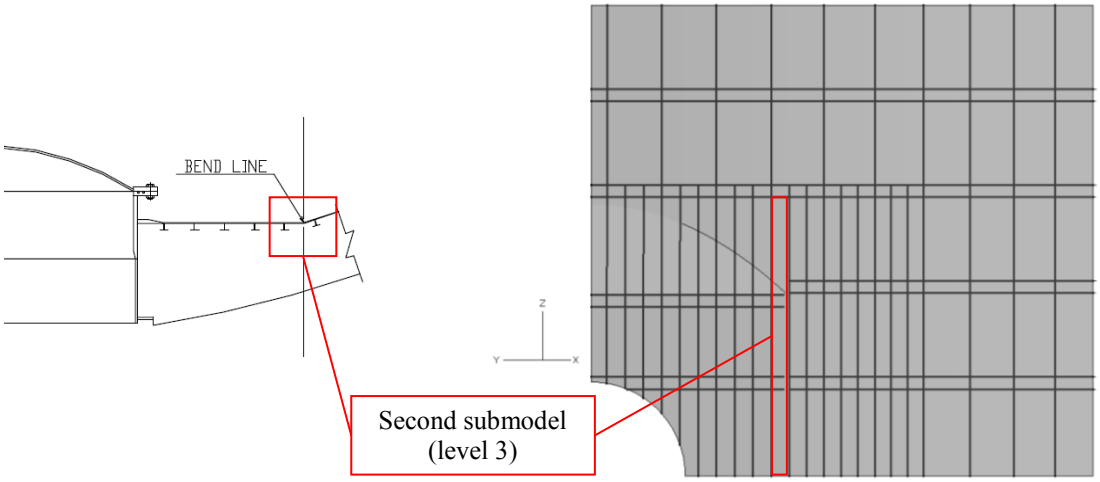

Figure 5. Left, excerpt from liner drawing in Hessheimer M.F. et al. (2003) showing a horizontal section through the E/H. Right, local liner model (level 2), where the location of the detailed liner model (level 3) is indicated.

LINER FAILURE CRITERIA

The uniaxial ultimate elongation (ε_u) was measured in tensile tests and the average value was concluded to be 0.33, see Hessheimer M.F. et al. (2003). The failure strain for the real structure is assumed to be reduced due to two factors in this study; welds and multi-axial stress state. In the pretest analysis for the Sandia 1:4 project, see Dameron R- A., et. al. (2000), these two factors is considered and it is concluded that the maximum reduction due to biaxial stress state is 50% (based on the Davis triaxiality factor *TF*) and the reduction due to welds is around 40% (based on tests).

Other factors, not captured by the FE-analyses, will also influence the liner failure. In Hessheimer M.F. et al. (2003) it is stated that the liner was grinded in connection with welding, which resulted in localized areas with thinner liner. Depending of the size of the reduction of the liner thickness, this fact could of course highly influence the initiation of liner failure. Another factor which could increase the strain level locally is large discrete concrete cracks in combination with friction between concrete and liner. This effect is studied in Anderson P. (2008b) and it is concluded that friction in combination with large concrete cracks could give elevated strain especially for thin liners, as for the containment scale model.

RESULTS AND EVALUATION

In this section the general results for the liner and the interacting structure near the equipment hatch (E/H) is presented. Focus is on liner strain and mechanisms generating elevated liner strain.

Displacement and contact

Figure 6 shows the radial displacement of the concrete inner surface in the studied region. The displacement is shown for the concrete part of the local model (level 2), where all nodes are restrained by the displacement in the global model. The maximum radial displacement (27 mm) agrees with the measured radial displacement in the E/H region, see Hessheimer M.F. et al. (2003). The average radial displacement around midheight, at an inner pressure of 1.29 MPa (3.3 pd), is around 20 mm according to the global analysis and this correspond to a maximum global strain of around 0.4% (radius = 5375 mm).

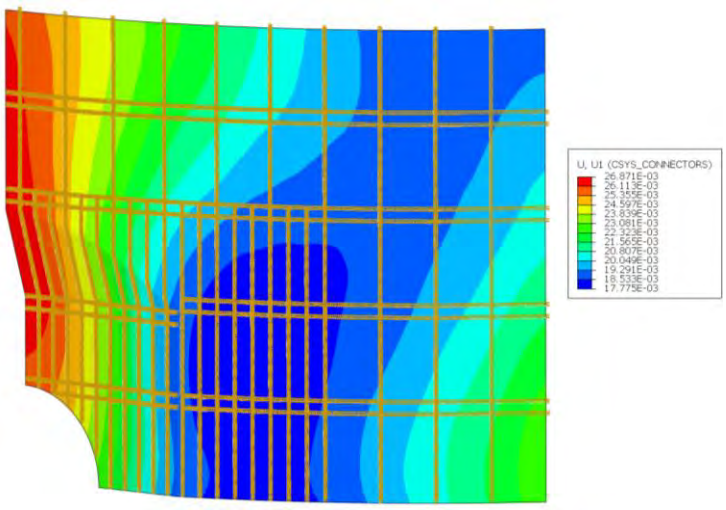

Figure 6. Concrete inner surface, radial displacement at 1.29 MPa (3.3 pd) in E/H region.

Figure 7 show the contact opening between liner and concrete shell. In general the liner is in contact with the concrete wall. However, in border lines between the E/H embossment and the general curved containment wall (outgoing folds), the liner will straighten out and separate from the concrete. This flexural behavior of the liner was also found in Anderson P. (2008a), where the same region was investigated. The size of the opening between concrete and liner depends on the shear stiffness in the vertical liner anchors. The analysis with high shear stiffness gives a maximum contact opening of around 2.3 mm. The analysis with low shear stiffness gives a maximum contact opening of 3.2 mm.

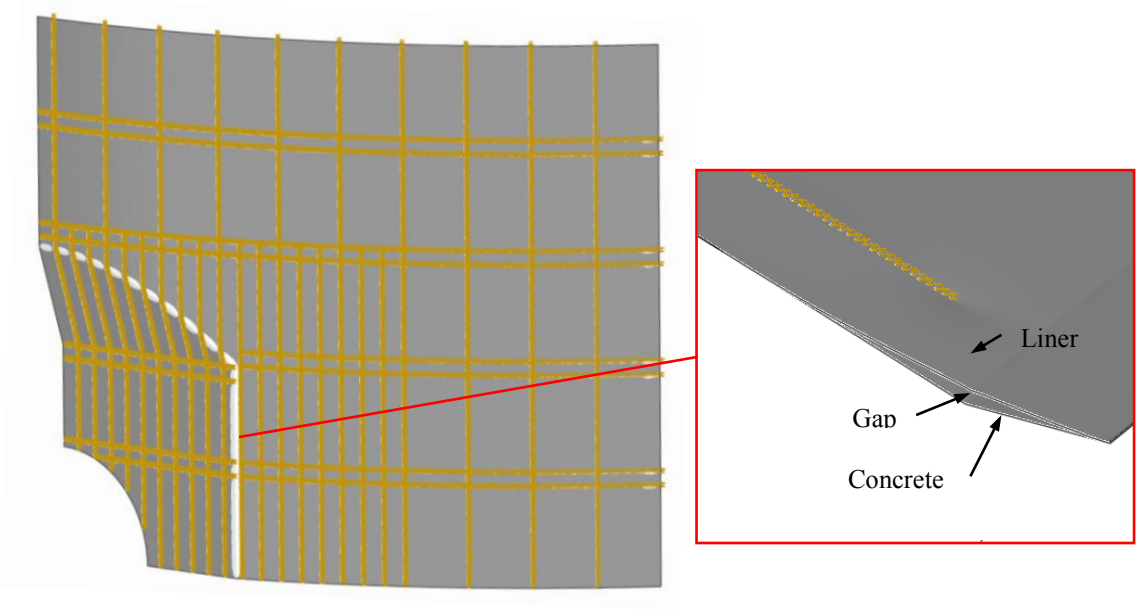

Figure 7. Concrete inner surface, separation between concrete and liner at 1.29 MPa (3.3 pd) in E/H region. White regions indicate where the liner has separated from the concrete.

The shear displacement in connectors representing the anchor close to the vertical fold is given in Figure 8. Results from analysis with both stiff and soft anchors are shown. The liner is sliding in the direction from the fold on both sides. The liner part that contains the fold can be seen as a week section and this causes an unbalance force in the anchor which causes the displacement in the anchors. If weaker shear stiffness is assumed, the anchor displacement increases.

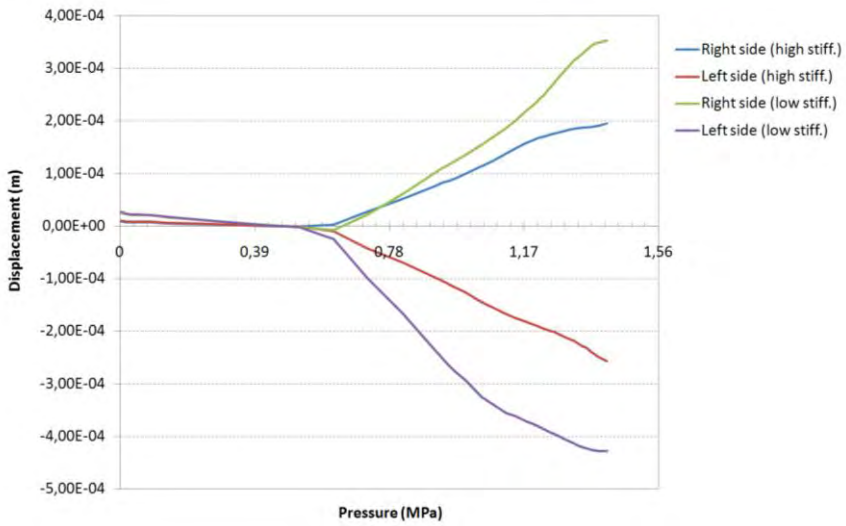

Figure 8. Liner anchor shear displacement near to vertical bend line (both sides of bend line at around level +5500).

Liner strain

Figure 9 shows the hoop strain at the inner concrete surface in the E/H region. Elevated strain can be seen in two regions (azimuth around 350º and around 5º) and the maximum strain in the hoop direction is around 1.5%. In the regions with elevated strain the horizontal reinforcement area is decreased. In the region close to the embossment (azimuth 300º to 350º) the horizontal reinforcement area is around 2.5 times the general reinforcement area. In the region just outside the embossment region (azimuth 350º to 5º and 285º to 300º) the horizontal reinforcement area is around 1.3 times the general reinforcement.

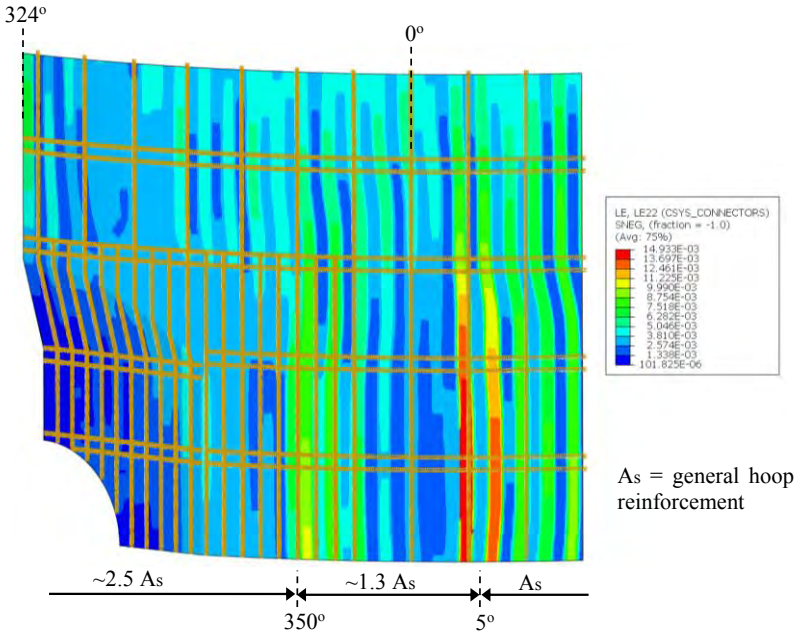

Figure 9 Concrete inner surface, strain at 1.29 MPa (3.3 pd) in hoop direction.

Figure 10 shows the liner strain in local model (level 2), where the liner is connected to the concrete by discrete connectors (see chapter Liner FE-models). Elevated strains can be seen in the same regions as shown in Figure 9 and the strain in these regions is around 0.8% (localized concrete strain is distributed between anchors). However, elevated strain can also be observed in the region close to the outgoing fold which is straightened out during pressurization (see displacement and contact above). Due to the flexural behavior when the liner is straightened out the strain will increase locally in the fold and close to the nearest anchor profile. To analyze the localized strain due to bending in the fold region, a detailed model with finer mesh is used (level 3).

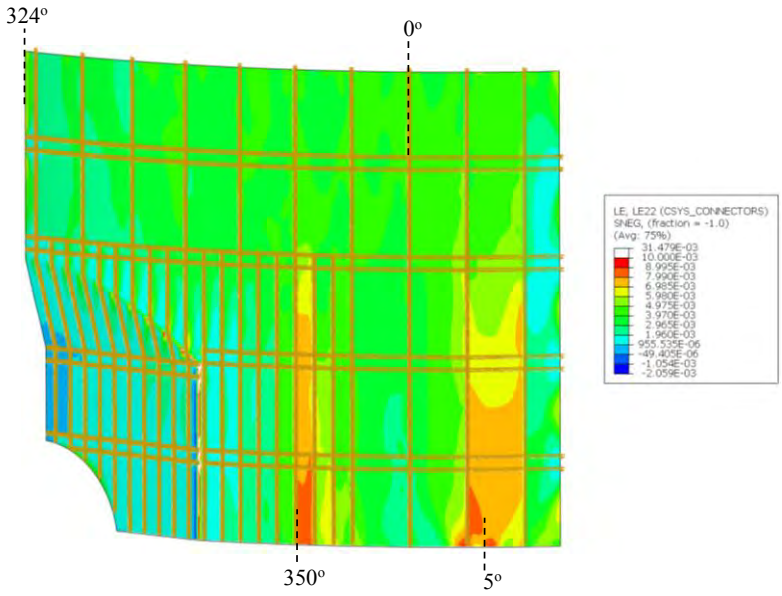

Figure 7.10 Liner strain at 1.29 MPa (3.3 pd) in hoop direction.

Figure 11 show hoop strain of the vertical fold analyzed by the detailed liner model (level 3). In the vertical fold the maximum tensile liner strain is around 5.7%. The highest strain values in the fold arise on the inside of the liner at the level of the horizontal stiffeners. The values presented here are given from the analysis with low anchor shear stiffness. High shear stiffness gives lower strain values (~ 4.6%).

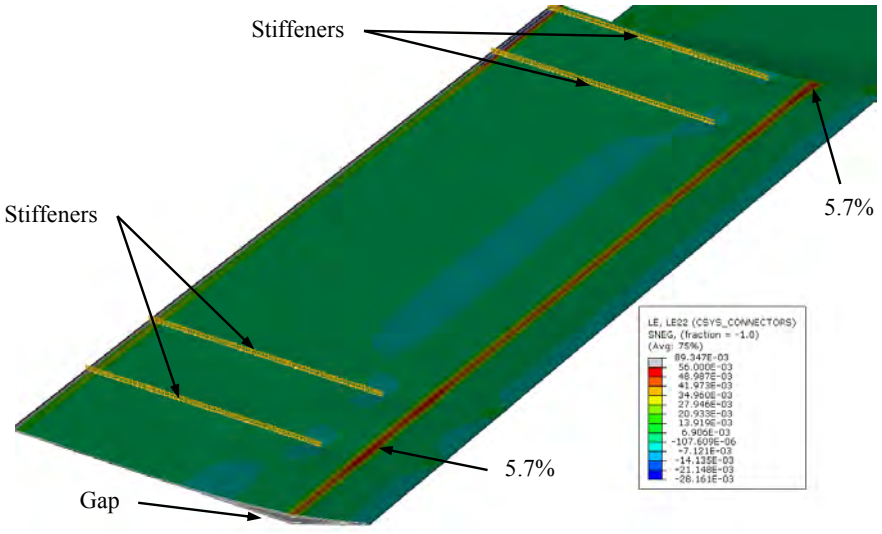

Figure 11. Detailed liner model, strain on liner inside at 1.29 MPa (3.3 pd) in hoop direction.

CONCLUSIONS

Three regions with elevated liner strain are found in this study (see Figure 7.10).

- Vertical fold between E/H embossment and general curved wall
- Along vertical line at azimuth ~ 350°
- Along vertical line at azimuth ~ 5°

The elevated strain along the vertical fold arises due to the flexural behavior when the liner is straightened out at high internal pressure. The strain level is concluded to depend on the shear stiffness in the vertical anchors. Analyzes with two different shear stiffness values are carried out and for the weak anchors the maximum tensile strain is 5.7% (see Figure 7.11). The maximum peak strain on the inside of the vertical fold is around 14 times (5.7/0.4) the average radial strain in the global analysis. The maximum strain in the vertical fold agrees with the location of tears found after the Sandia ¼ test (see Figure 1, tear #7, #12, #13 and #15).

The elevated strain found at azimuth 5° and 350° corresponds to the elevated concrete strain. The elevated concrete strain is concluded to be caused by the reduced hoop reinforcement. The maximum tensile liner strain found in this region is around 0.8% (see Figure 7.10). The elevated strain at azimuth 5° agrees with the tears found after the Sandia ¼ test (see Figure 1, tear #1 and #8).

The uni-axial failure strain is in this paper assumed to be reduced by two factors, biaxial stress state and welds. The liner failure strain estimated in in this paper is around 10% (0.33x0.5x0.6). The maximum liner strain found in analyses presented in this paper do not reach the estimated failure strain. However, different factors not considered in the FE-models could generate elevated strain. As stated in Hessheimer M.F. et al. (2003), the liner thickness was reduced locally due to grinding which could localize the strain in these regions. Also, in Anderson P. (2008b) it is concluded that large concrete cracks could give elevated strain, especially for thin liners, due to the friction between liner and concrete.

REFERENCES

Anderson P (2008a), “Analytic study of the steel liner near the equipment hatch in a 1:4 scale containment model”, Nuclear Engineering and Design, vol 238. p 1641-1650.

Anderson P (2008b), “Concentration of plastic strains in steel liners due to concrete cracks in the containment wall”, International Journal of Pressure Vessels and Piping, vol 85. p 711-719.

Dameron R- A., Zhang, L., Rashid Y. R. and Vargas M. S. (2000), “Pretest Analysis of a 1:4-Scale Prestressed Concrete Containment Vessel Model”, NUREG/CR-6685.

Hessheimer M. F. et al. (2003), “Overpressurization test of a 1:4-Scale prestressed concrete containment vessel model”, NUREG/CR-6810, U.S. NRC.

Horschel D.S. et al. (1988), “Design, construction, and instrumentation of a 1/6-scale reinforced concrete containment building” NUREG/CR-5083, U.S. NRC.

ISP-48 (2005), “International Standard Problem 48 Containment Capacity”, Phase 1-3, OECD.